J|A|C|S
ARTICLES
Published on Web 07/10/2002

Oligopeptides with Homochiral Sequences Generated from Racemic Precursors that Spontaneously Separate into Enantiomorphous Two-Dimensional Crystalline Domains on Water Surface

Isabelle Weissbuch,*,† Gérard Bolbach,‡ Helmut Zepik,† Edna Shavit,† Mao Tang,† Joseph Frey,† Torben R. Jensen,§ Kristian Kjaer,§ Leslie Leiserowitz,*,† and Meir Lahav*,†

Contribution from the Department of Materials and Interfaces, The Weizmann Institute of Science, 76100-Rehovot, Israel, Laboratoire de Chimie Structurale Organique et Biologique, Université Pierre et Marie Curie, 75252 Paris Cedex 05, France, and Materials Research Department, Risø National Laboratory, 4000 Roskilde, Denmark

Received February 21, 2002

Abstract: The feasibility of generating oligopeptides with homochiral sequence via lattice-controlled polymerization of racemic mixtures of precursor molecules that undergo spontaneous segregation into two-dimensional (2-D) enantiomorphous domains at the air−aqueous solution interface was analyzed. For model systems, we studied the polymerization reaction within 2-D crystalline domains of mixtures of (*R*,*S*)-N^{ϵ}-stearoyl-thio-lysine with ∼10% (*R*,*S*)-N^{ϵ}-stearoyl-lysine, and (*R*,*S*)-N^{α}-carboxyanhydride of N^{ϵ}-stearoyl-lysine. According to in situ grazing incidence X-ray diffraction (GIXD) measurements at the air−water interface, the molecules form 2-D crystallites packing by translation symmetry only. Oligopeptides 4−6 units long were obtained at the air−solution interface after injection of an appropriate catalyst into the subphase. The course of the chemical transformations was monitored by GIXD. The distribution of the diastereoisomeric oligopeptides was determined by matrix-assisted laser-desorption ionization time-of-flight (MALDI-TOF MS) mass spectrometry on samples prepared from precursor molecules enantioselectively labeled with deuterium. The experimental relative abundance of oligopeptides with homochiral sequence was found to be larger than that calculated for a theoretical random process, yielding an excess by a factor of 2.5−3.5 for the tetra- to hexapeptides. The present studies may be relevant for probing the role that might have been played by ordered clusters at interfaces for the generation of homochiral oligopeptides under prebiotic conditions.

Introduction

The question, how homochiral biopolymers might have been formed from racemic mixtures in prebiotic times, has long intrigued naturalists interested in the origin of life.[1−5] It comprises two principle aspects, first the formation, from racemic monomers, of polymers with homochiral sequence and second the prevalence of the homochiral polymers of only one single-handedness. The first aspect of this general question will be addressed here.

Polymerization reactions of racemic monomers in isotropic media would yield, however, polymers with a random sequence of left- and right-handed units. For such a random process the probability of obtaining polymers with homochiral sequence becomes negligible with increasing polymer length.

The spontaneous segregation of racemic mixtures of certain amphiphilic molecules into enantiomorphous two-dimensional (2-D) crystalline domains at solid and liquid interfaces has been demonstrated by applying surface-sensitive analytical methods such as grazing incidence X-ray diffraction[6,7] (GIXD) on water surface and scanning probe methods (SPM) on solid support.[8−10]

In the present study we focused on the question whether a lattice-controlled polymerization of activated racemic α-amino acids within such enantiomorphous domains at the air−water

* To whom correspondence should be addressed. E-mail addresses: isabelle.weissbuch@weizmann.ac.il; leslie.leiserowitz@weizmann.ac.il; meir.lahav@weizmann.ac.il.
† The Weizmann Institute of Science.
‡ Université Pierre et Marie Curie.
§ Risø National Laboratory.

(1) Franck, P.; Bonner, W. A.; Zare, R. N. In *Science in 21st Century*; Keinan, E., Schecter, I., Eds.; Wiley−VCH: 2000; p 175.
(2) Joyce, F. F.; Visser, G. M.; van Boeckel, C. A. A.; van Boom, J. H.; Orgel, L. E.; van Westrenen, J. *Nature* **1988**, *310*, 602.
(3) Brack, A.; Spach, G. *Origins Life* **1981**, *11*, 135.
(4) Bolli, M.; Micura, R.; Eschenmoser, A. *Chem. Biol.* **1997**, *4*, 309.
(5) Siegel, J. S. *Chirality* **1998**, *10*, 24.
(6) Kuzmenko, I.; Rapaport, H.; Kjaer, K.; Als-Nielsen, J.; Weissbuch, I.; Lahav, M.; Leiserowitz, L. *Chem. Rev.* **2001**, *101*, 1659.
(7) Weissbuch, I.; Kuzmenko, I.; Berfeld, M.; Leizerowitz, L.; Lahav, M. *J. Phys. Org. Chem.* **2000**, *13*, 426−434.
(8) de Feyter, S.; Grim, P. C. M.; Rucher, M.; Vanoppen, P.; Meiners, C.; Sieffert, M.; Valiaveettil, S.; Mullen, K.; de Schryver, F. C. *Angew. Chem.* **1998**, *37*, 1223.
(9) Boringer, M.; Morgerstern, K.; Schnider, W. D.; Berndt, R. *Angew. Chem., Int. Ed.* **1999**, *38*, 821.
(10) Stevens, F.; Dyer, D. J.; Walba, D. M. *Angew. Chem., Int. Ed. Engl.* **1996**, *35*, 900.

10.1021/ja0259943 CCC: $22.00

Scheme 1

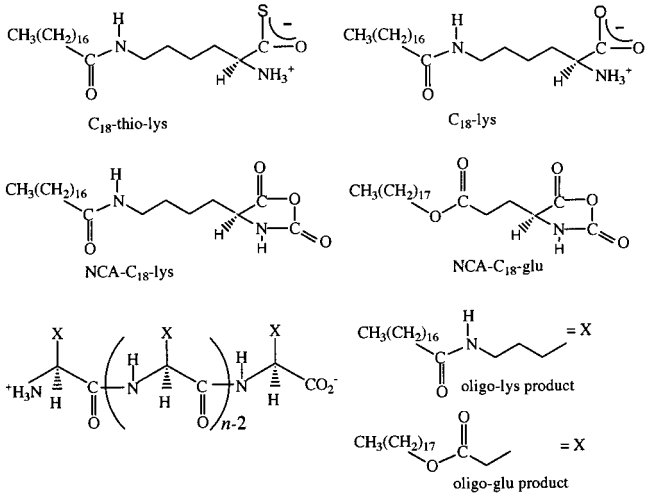

interface might provide a route for the formation of an excess of oligopeptides of homochiral sequence.

Previous reports have shown that amphiphilic molecules in Langmuir monolayers undergo polymerization reactions.[11,12] Recently we have reported the spontaneous separation of racemic mixtures of long-chain derivatives of lysine [C_nH_{2n+1}−CO−NH−$(CH_2)_4CH(NH_3^+)CO_2^-$, $n = 15-21$] into enantiomorphous 2-D crystals at the air−water interface.[13] The molecules within such domains were induced to pack by translation symmetry only by virtue of the (N)H···O(C) intermolecular hydrogen bonding between the amide groups and between the zwitterionic α-amino acid moieties. By contrast, the related amphiphiles that lack the amide group self-assemble into a racemic-type of arrangement with molecules related by glide symmetry.

On the basis of the above considerations, two model systems were designed to both self-assemble into enantiomorphous 2-D domains and undergo lattice-controlled polymerization reaction: mixtures of racemic N^{ϵ}-stearoyl-thio-lysine (C_{18}-thio-lys)[14] with N^{ϵ}-stearoyl-lysine (C_{18}-lys), and racemic N^{α}-carboxyanhydride of N^{ϵ}-stearoyl-lysine (NCA-C_{18}-lys) (Scheme 1). The packing arrangements of their self-assembled 2-D crystallites at the air−water interface were determined by GIXD using synchrotron radiation. The diastereoisomeric distribution of the oligopeptide products starting from racemic monomers enantioselectively labeled[15−17] with deuterium was determined by matrix-assisted laser-desorption ionization time-of-flight mass spectrometry (MALDI-TOF-MS).[18]

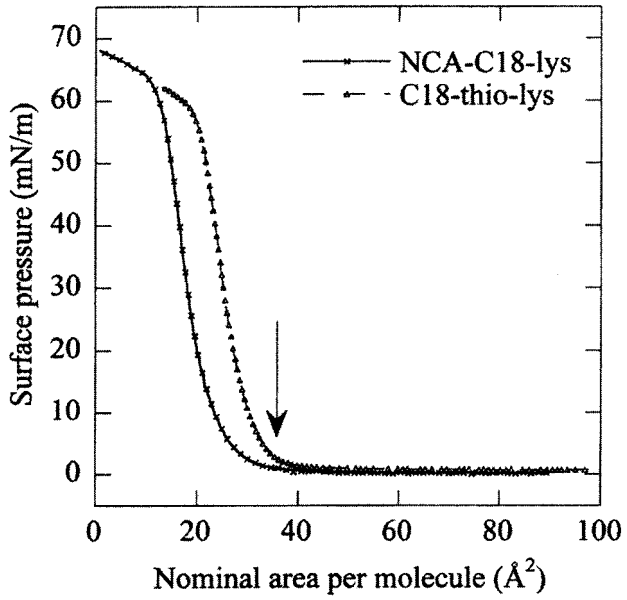

Figure 1. Surface pressure − nominal molecular area ($\pi - A$) isotherms measured from (*R*)-, or (*S*)- and (*R*,*S*)--amphiphiles on water surface at 20 °C: (△) −C_{18}-thio-lys and (×) −NCA-C_{18}-lys. The arrow represents the point on the isotherms where the GIXD measurements were performed.

Scheme 2

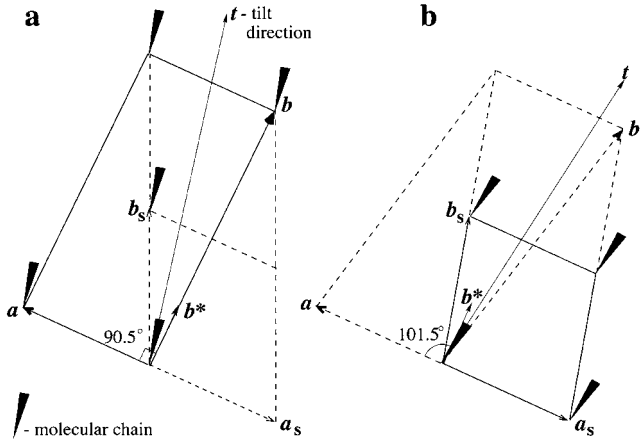

Results and Discussion

C_{18}-thio-lys System: GIXD of (*R*)-, or (*S*)- and (*R*,*S*)-C_{18}-thio-lys on Water. The 2-D packing arrangements were determined by GIXD on samples prepared by spreading chloroform solutions of the amphiphiles on water surface, at 4 °C, for a nominal molecular area of 35 Å^2. According to the surface pressure−area isotherms, (Figure 1), this state of the monolayer corresponds to a coverage of ∼75% with no increase in the surface pressure.

The GIXD patterns measured from chemically pure (*R*)- or (*S*)- and (*R*,*S*)-C_{18}-thio-lys are very similar, as seen from the two-dimensional contour plots of scattered intensity $I(q_{xy},q_z)$ in Figure 2a,b. From the q_{xy} positions of the observed Bragg peaks, with assigned Miller indices as in Figure 2a,b, we derived an oblique unit cell, of dimension $a_s = 4.9$ Å, $b_s = 5.6$ Å, $\gamma_s = 115.5°$, area $= a_s b_s \sin\gamma_s = 25.2$ Å^2, containing one molecule.

This unit cell can be transformed into a pseudo-rectangular cell ($a = a_s$ and $b = \boldsymbol{a}_s + 2\boldsymbol{b}_s$) of dimension $a = 4.9$ Å, $b = 10.2$ Å, $\gamma = 89.5°$, containing two molecules, as shown in Scheme 2a. The molecular hydrocarbon chains are tilted from

(11) Fukuda, K.; Shibasaki, Y.; Nakahara, H.; Liu, M. *Adv. Colloid Interface Sci.* **2000**, *87*, 113.
(12) Shibata, A.; Hashimura, Y.; Yamashita, S.; Ueno, S.; Yamashita, T. *Langmuir* **1991**, *7*, 2261.
(13) Weissbuch, I.; Berfeld, M.; Bouwman, W.; Kjaer, K.; Als-Nielsen, J.; Lahav, M.; Leiserowitz, L. *J. Am. Chem. Soc.* **1997**, *119*, 933.
(14) Note that this compound was chosen since α-amino thio acids are reactive precursors for the formation of peptide bonds and they have been suggested as prebiotic precursors (see Maurel, M. C.; Orgel, L. E. *Origins Life Evol. Biosphere* **2000**, *30*, 423). Moreover, sulfur-activated α-amino acids might have been formed under primordial conditions at surfaces of iron−sulfur minerals (see Huber, C.; Wächtershäser, G. *Science* **1997**, *276*, 245).
(15) Addadi, L.; Gati, E.; Lahav, M.; Leiserowitz, L. *Isr. J. Chem.* **1977**, *15*, 116.
(16) Blocher, M.; Hitz, T.; Luisi, P. L. *Helv. Chim. Acta* **2001**, *84*, 842.
(17) Zepik, H.; Shavit, E.; Tang, M.; Jensen, T. R.; Kjaer, K.; Bolbach, G.; Leiserowitz, L.; Weissbuch, I.; Lahav, M. *Science* **2002**, *295*, 1266.
(18) Karas, M.; Bachmann, D.; Hillenkamp, F. *Anal. Chem.* **1985**, *57*, 2935.

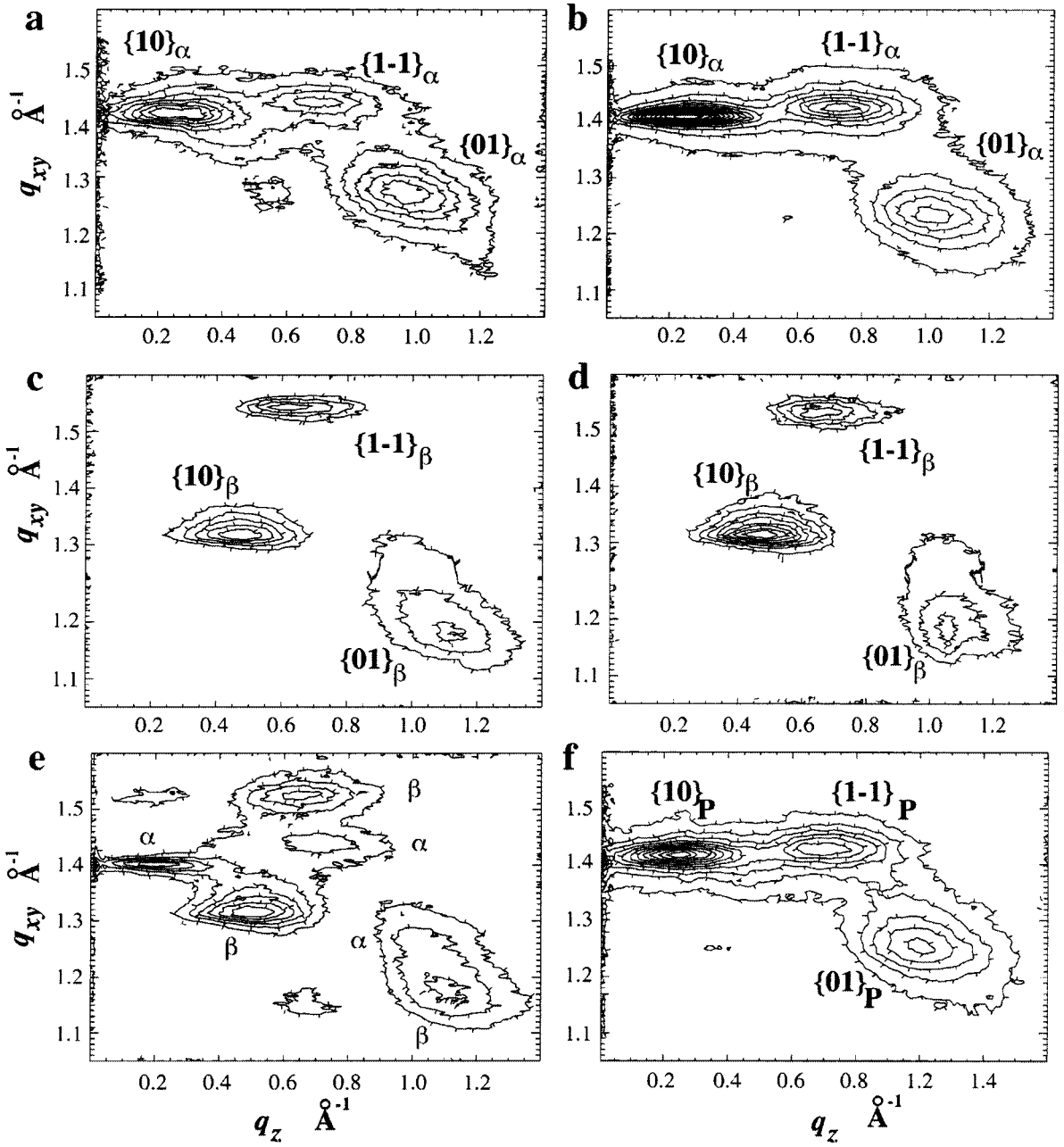

Figure 2. GIXD patterns $I(q_{xy}, q_z)$ of the self-assembled 2-D crystallites of C_{18}-thio-lys on water at 4 °C, where q_{xy} and q_z are horizontal and vertical components of the X-ray scattering vector: (a) Chemically pure enantiomeric *R*, (*S* yielded an almost identical pattern), (b) chemically pure racemate *R*,*S*, (c) mixture of (*S*)-C_{18}-thio-lys with 10% (*S*)-C_{18}-lys, (d) mixture of (*R*,*S*)-C_{18}-thio-lys with 10% (*R*,*S*)-C_{18}-lys, (e) pure racemate kept at 4 °C for 3 days, and (f) 2 h after catalyst addition into the subphase of (a−e). Note that the reflections are indexed with (*h*,*k*) Miller indices with subscript α, *β*, or P, corresponding to the α- and *β*-phases of the monomer and product phase, respectively.

the normal to the water surface by 40.5° with an azimuthal angle of 13.3° from the *b** reciprocal lattice vector (Scheme 2a).

According to these results, in the (*R*) or (*S*) 2-D crystallites the two molecules should be related by translation in a centered cell. In contrast, (*R*,*S*)-C_{18}-thio-lys forms racemic (*R*,*S*) 2-D crystallites in view of the almost rectangular unit cell. Since the molecular chains are not tilted along the *b* axis, the two molecules in the unit cell are crystallographically independent, with their long-hydrocarbon chains related by pseudo-glide symmetry to form a pseudo-herringbone motif.[19] To satisfy this requirement, the long hydrocarbon chain should not be coplanar with the secondary amide −CO−NH− group running parallel to the *a* axis to achieve intermolecular hydrogen bonding along this axis.

Molecular models constructed using the CERIUS[2] computational package[21] were refined using the X-ray structure factor least-squares program SHELX-97,[22] but applied to 2-D crystals, to yield a reasonable fit between the observed and calculated Bragg rod intensity profiles (Figure 3a). The proposed 2-D

(19) This pseudo-glide symmetry may be considered in terms of a glide plane that is not exactly perpendicular to the water surface. Indeed, such a motif was invoked to explain the GIXD patterns measured from 2-D crystallites of long-chain alcohol amphiphiles on water.[20]

(20) Wang, J. L.; Leveiller, F.; Jacquemain, D.; Kjaer, K.; Als-Nielsen, J.; Lahav, M.; Leiserowitz, L. *J. Am. Chem. Soc.* **1994**, *116*, 1192.
(21) Cerius^2, BIOSYM/Molecular Simulations, Inc.: San Diego, CA, 1995.
(22) Sheldrick, G. M. *SHELXL97*, Program for the Refinement of Crystal Structures; University of Göttingen, Germany, 1997.

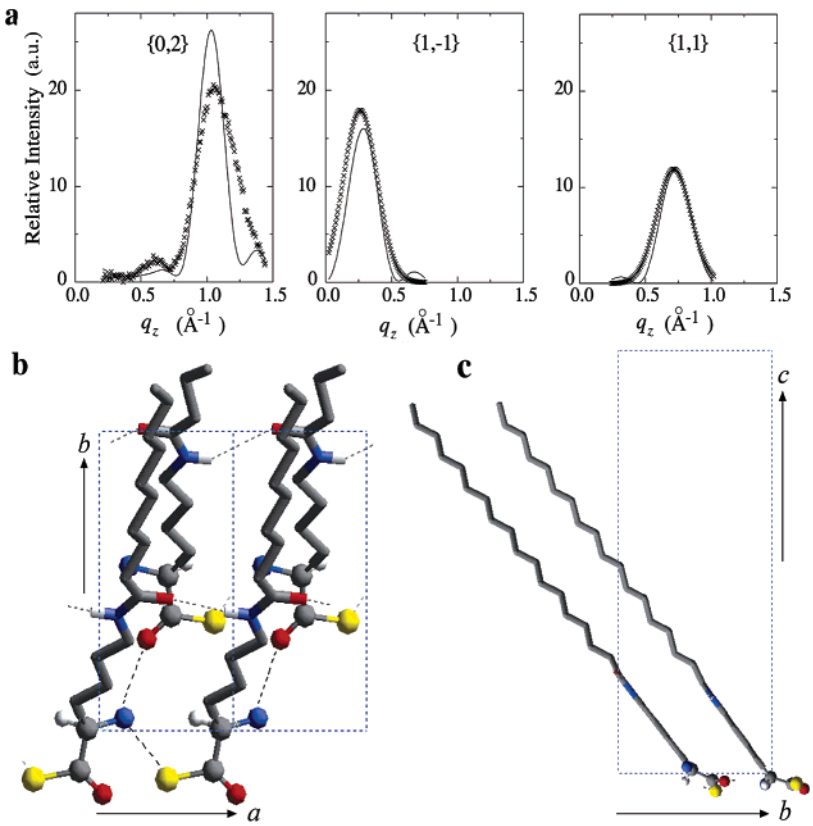

Figure 3. Structure determination of the racemic-type (α-phase) of (*R*,*S*)-C_{18}-thio-lys 2-D crystallites: (a) Measured (×) and calculated (—) Bragg rod intensity profiles, $I(q_z)$, of the {0,2}, {1,−1}, and {1,1} reflections corresponding to the pseudo-rectangular representation of the unit cell, (b) and (c) The 2-D packing arrangement viewed perpendicular and parallel to the water surface, respectively. The color code is: C (gray), H (white), N (blue), O (red), S (yellow). For clarity, only part of the hydrocarbon chains is shown in (b). Note that the length of the *c* axis is arbitrary.

packing arrangement containing the (*R*) and (*S*) molecules related by pseudo-glide symmetry along the *b* axis and with their long chains forming a herringbone motif, is shown in Figure 3b,c viewed normal and parallel to the water surface.

We note here the difference between the unit cell determined for the 2-D crystallites of (*R*,*S*)-C_{18}-thio-lys (cell dimension $a = 4.9$ Å, $b = 10.2$ Å, $\gamma = 89.5°$) and that of the corresponding (*R*,*S*)-C_{18}-lys. For the latter system, the unit cell in the *pseudo*-rectangular representation has dimension $a = 4.9$ Å, $b = 9.6$ Å, $\gamma = 100.7°$, where the γ angle is sufficiently different from 90° to exclude packing via glide symmetry, thus favoring molecular packing by translation symmetry only.[23] Thus, C_{18}-thio-lys is not isostructural with the corresponding C_{18}-lys.

To induce C_{18}-thio-lys to pack only via translation, implying a spontaneous separation into enantiomorphous domains, we prepared mixtures of C_{18}-thio-lys with ∼10−15% mol C_{18}-lys. The GIXD patterns measured from such mixtures of the corresponding (*R*)-, or (*S*)- and (*R*,*S*)-amphiphiles (Figure 2c,d) are again very similar to one another but belong to a different crystalline phase. These patterns show not only changes in the positions of the Bragg peaks as compared to those measured from the chemically pure amphiphiles but also significantly different Bragg rod intensity profiles. The derived oblique unit cell ($a = 4.9$ Å, $b = 5.5$ Å, $\gamma = 104.5°$, area = 26.2 Å^2) contains one molecule tilted from the normal to the water surface by 43.6°, making an azimuth angle of 7.5° with *b** (Scheme 2b). This unit cell can be transformed into a centered cell of dimension $a = 4.9$ Å, $b = 10.9$ Å, $\gamma = 101.5°$, containing two molecules but with $\gamma \neq 90°$, thus very different from being a pseudo-rectangular cell. Consequently, the molecules must certainly pack by translation symmetry only, similar to the packing of the corresponding C_{18}-lys. The derived 2-D packing motif is shown in Figure 4. These results indicate that the presence of the C_{18}-lys additive induced the translation motif via a hydrogen-bonding stabilization that can also prevent enantiomeric disorder of the headgroups.

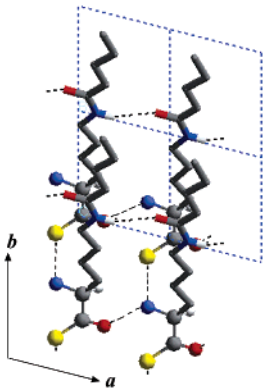

Figure 4. Proposed packing arrangement of the enantiomorphous-type of 2-D crystallites (*β*-phase) self-assembled from the mixture of (*R*,*S*)-C_{18}-thio-lys with 10% (*R*,*S*)-C_{18}-lys, viewed normal to the water surface.

(23) Note that the unit cell of C_{18}-lys is very similar to that of the *ac* layer in the 3-D crystal of glycine[24] due to the N−H···O hydrogen bonding. In 3-D crystals of (*R*,*S*)-methionine[25] and α-aminobutyric acid,[26] where the molecules within the hydrogen-bonded layer are related by glide symmetry, the corresponding unit cell is rectangular. A similar rectangular unit cell was measured for the 2-D crystallites of racemic α-aminostearic acid.[13]

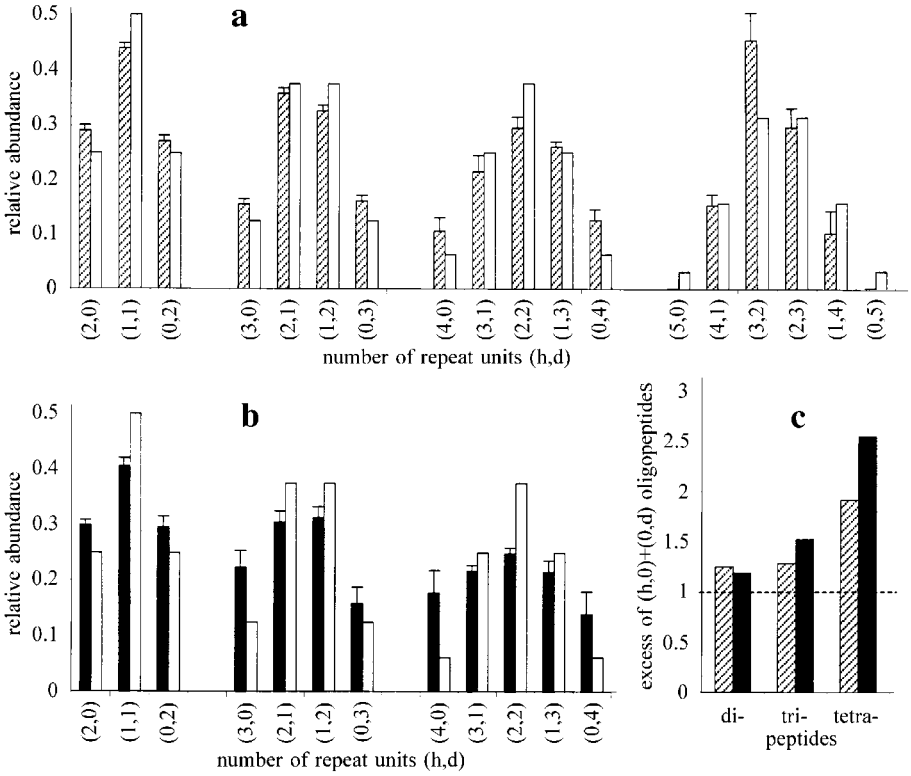

Figure 5. (a, b) MALDI-TOF MS analysis of the oligopeptides obtained from racemic C_{18}-thio-lys. The histograms show the experimental relative abundance of each oligopeptide (filled bars) obtained after the polymerization at the air−aqueous solution interface from: (a) the α-phase of pure (*R*,*S*)-C_{18}-thio-lys (lined) and (b) the *β*-phase of *R*,*S* C_{18}-thio-lys mixed with 10% *R*,*S*-C_{18}-lys (filled). Note that experiments performed at 4 and 20 °C gave similar results. The experimental distributions are compared with the theoretical values (unfilled bars) calculated from a binomial distribution of the *R* and *S* repeat units in a random process. For the notation (*h*,*d*) code see the Experimental Section. No substantial isotope effect was observed on interchanging the isotope labeling of the two enantiomers. The error bars were determined from different experiments on a sample and from different samples; (c) The excess of oligopeptides with homochiral sequence [(*h*,0) + (0,*d*)] (for definition see text and Experimental Section) is shown for the di-, tri-, and tetrapeptides obtained from the polymerization reactions of the α (lined)- and *β* (filled)-monomer phases. The horizontal dashed-line represents an excess value equal to unity.

The coexistence of the two crystalline phases, the α-form (Figure 2b) of the pure C_{18}-thio-lys and the *β*-form (Figure 2d) of the (C_{18}-lys:C_{18}-thio-lys) mixture, was observed (Figure 2e) when a solution of the chemically pure racemic C_{18}-thio-lys was kept at 4 °C for 2−3 days prior to sample preparation.[27]

Monitoring the Polymerization of (*R*,*S*)-C_{18}-thio-lys by GIXD. C_{18}-thio-lys polymerizes only in the presence of a suitable catalyst. Therefore, after measurement of the GIXD patterns of the 2-D crystallites on pure water, the I_2/KI catalyst[28] was injected into the subphase beneath the monolayer and the reaction monitored by GIXD. The formation of the oligopeptide products induced a relatively small but consistent change in the q_z positions of the Bragg rods of the α-phase (Figure 2b), as shown in Figure 2f after 2 h of reaction. The derived unit cell is, in pseudo-rectangular representation, of dimension $a = 4.9$ Å, $b = 9.97$ Å, $\gamma = 89.0°$. Interestingly, the GIXD pattern of the oligopeptides is the same, when starting from a mixture of α and *β* phases (Figure 2e) of the reactants. This result, however, does not imply that in all cases the oligopeptides have the same enantiomeric composition.

Enantiomeric Composition of the Oligopeptide Products. MALDI-TOF MS analysis was used to determine the number of the *R* and *S* units within each oligopeptide molecule obtained in the polymerization reaction. For this purpose, one of the reactant enantiomers was labeled with a per-deuterated stearoyl chain yielding a mass difference per peptide unit of $\Delta m/z = 35$.

According to the MALDI-TOF MS analysis, samples prepared by polymerization of pure (*R*,*S*)-C_{18}-thio-lys contain a mixture of di- to pentapeptide products of various composition. Although we cannot differentiate between diastereomeric oligopeptides containing the same number of *R* and *S* units, the method allows us to differentiate enantiomers of both homochiral and heterochiral oligopeptides.

For oligopeptides of the same length, the observed ion intensity in the MALDI-TOF spectra and the amount of molecules are reliably proportional. The chemical properties of such oligopetides are similar, and their ionization efficiencies are expected to be identical. In addition, their masses and velocities are very close, involving a very similar detection efficiency in the TOF mass spectrometer. We express the composition of the oligopeptides in terms of a relative abundance for molecules of each length. The relative abundance of oligopeptide (*h*,*d*), where *h* is the number of *S*(unlabeled) peptide units and *d* the number of *R*(deuterated) units, was obtained via the division of the intensity of all the ions corresponding to each molecule by the intensity of the ions from all the molecules of the same length (see Experimental section).

The MALDI-TOF MS analysis was performed on samples collected from the air−aqueous solution interface 2 h after the

(24) Legros, J.-P.; Kvick, A. *Acta Crystallogr.* **1980**, *B36*, 3052.
(25) Mathieson, A. M. *Acta Crystallogr.* **1952**, *5*, 332.
(26) Nakata, K.; Takaki, Y.; Sakurai, K. *Acta Crystallogr.* **1980**, *B36*, 504.
(27) This result is due to partial hydrolysis of C_{18}-thio-lys to C18-lys.
(28) Sheehan, J. C.; Johnson, D. A. *J. Am. Chem. Soc.* **1952**, *74*, 4726.

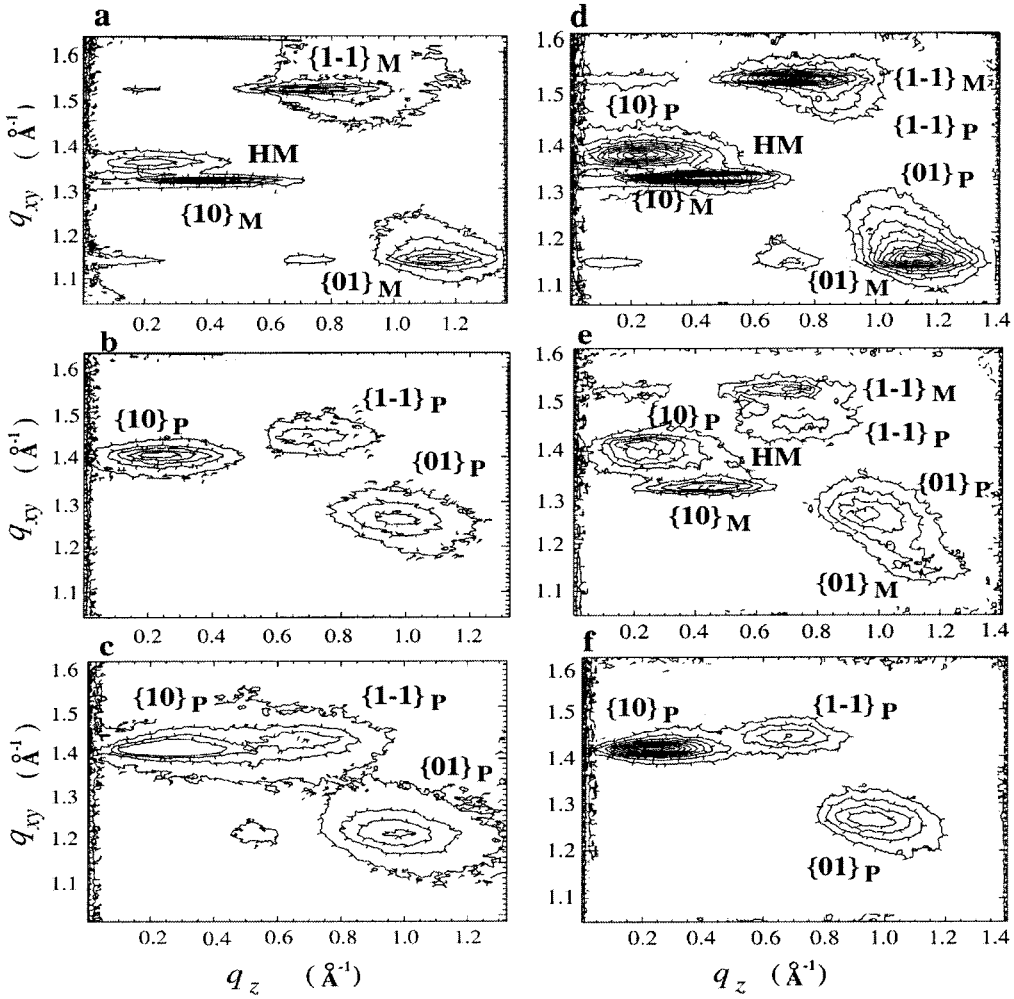

Figure 6. The GIXD patterns, shown as 2-D intensity contour plots $I(q_{xy},q_z)$, measured from self-assembled monolayers of: (a, b) enantiomeric *S*-, spread at 4 °C on water and on 5 mM nickel acetate aqueous solution, (*R*- yielded an almost identical pattern); (c) racemic NCA-C_{18}-lys spread at 4 °C, or at RT, on water, or on 5 mM nickel acetate aqueous solution, (d−f) enantiomeric (*S*)-NCA-C_{18}-lys spread on water at RT and cooled after 1 h to 4 °C (shown in (d)), followed by injection of the catalyst into the water beneath the film in two steps (shown in (e) and (f) after each injection). The Bragg peaks are labeled $\{h,k\}$ Miller indices with subscripts **M**, denoting the monomer phase, and **P** the product phase. The peak labeled **HM** belongs to the C_{18}-lys phase.

catalyst was injected beneath the 2-D crystallites. The relative abundance of various oligopeptides containing up to five units obtained from the α-phase of pure (*R*,*S*)-C_{18}-thio-lys (filled bars) is shown in Figure 5a together with the corresponding values calculated assuming a binomial distribution (unfilled bars) of the *R* and *S* repeat units (see Experimental Section). The di-, tri-, and tetrapeptides with homochiral sequence, labeled (*h*,0) and (0,*d*), have a relative abundance somewhat higher than the theoretical values. Homochiral pentapeptides (labeled (5,0) and (0,5) in Figure 5a) were not observed from the α-phase.

The relative abundance of oligopeptides obtained from the mixtures of (*R*,*S*)-C_{18}-thio-lys with 10% C_{18}-lys packing in the *β*-phase is shown in Figure 5b. In such samples we obtained only up to tetrapeptides, presumably since the C_{18}-lys additive acted as a polymerization terminator. However, the distribution of the tri- and tetrapeptides is wing-weighted rather than center-weighted in comparison with the corresponding theoretical values and those of the α-phase. In other words, the oligopeptides with homochiral sequence were obtained with higher relative abundance for the *β*-phase.

We express the excess of oligopeptides with homochiral sequence by normalizing the experimental relative abundance of oligopeptides $[(h,0) + (0,d)]$ to that calculated for a random process. Values larger than unity of this excess can provide a measure of the departure of the system from a random polymerization process. The experimental excess (Figure 5c) of di-, tri-, and tetrapeptides with homochiral sequences obtained from the two starting α- and *β*-phases is systematically larger for the *β*-phase, especially for the tetrapeptides. These results indicate that the packing arrangement of the starting crystalline phase exerts some control on the polymerization pathway. According to the packing arrangement of the α-phase that incorporates a possible intramolecular disorder due to the switch between the S and O atoms of the CSO^- group (Figure 3b), the reaction occurs presumably between molecules related by glide and by translation symmetry, with some preference for the latter. The packing arrangement of the *β*-phase implies spontaneous separation into enantiomorphous domains. However, the experimental excess of oligopeptides with homochiral sequence is not as high as may be expected. This result may be due to possible enantiomeric disorder present within the homochiral domains or due to reactions occurring at the line boundaries of the domains or in the noncrystalline regions of the film. One way to lessen the degree of enantiomeric disorder within the homochiral domains is to select amphiphiles with more rigid headgroups. Therefore we made use of NCA-C_{18}-

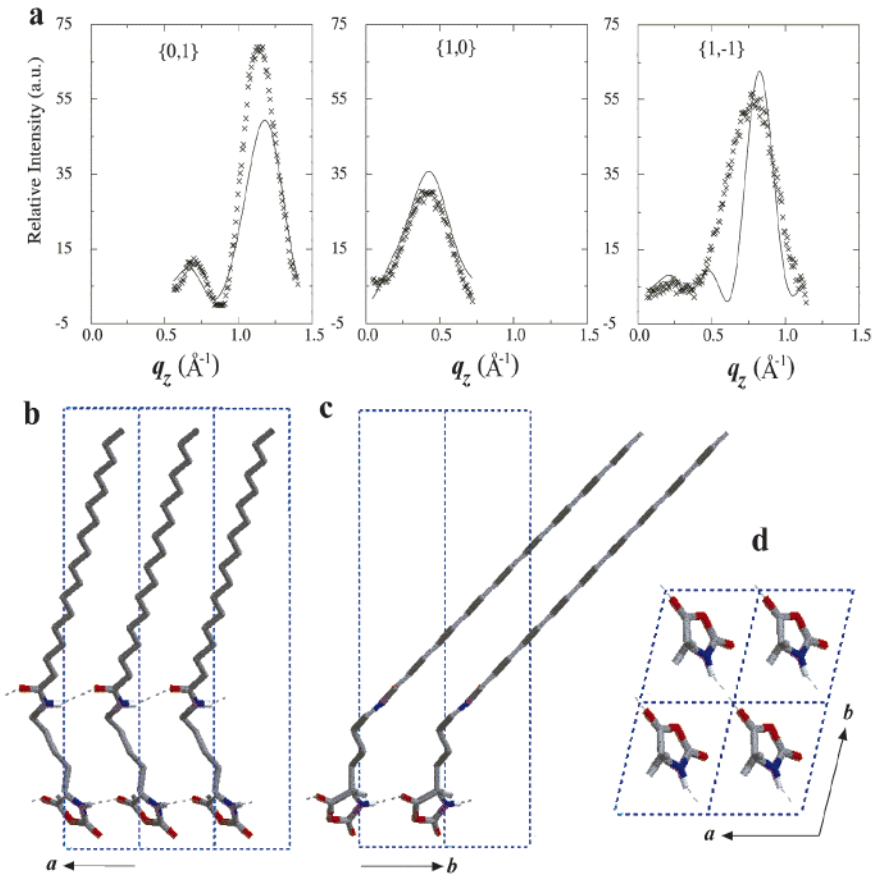

Figure 7. Structure determination of the enantiomeric (*R*)- or (*S*)-NCA-C_{18}-lys 2-D crystallites: (a) Measured (×) and calculated (—) Bragg rod intensity profiles, $I(q_z)$, corresponding to the {1,−1}, {1,0}, and {0,1} reflections, (b−d) The 2-D packing arrangement viewed parallel (along the *b* and *a* axes) and perpendicular to the water surface, respectively. For clarity, only the carboxyanhydride five-membered rings are shown in (d).

lys (Scheme 1) as a second model system, since the polymerizable *N*-carboxyanhydride headgroup is rigid.

NCA-C_{18}-lys System: GIXD of (*R*)- or (*S*)-NCA-C_{18}-lys on Water. Crystalline 2-D domains of enantiomerically pure NCA-C_{18}-lys were obtained by spreading chloroform solutions on water subphase at 4 °C for a nominal molecular area of 35 Å^2 corresponding to the state indicated with an arrow in the surface pressure − area isotherms (Figure 1). The GIXD measurements show the presence of two phases (Figure 6a). The major crystalline phase, composed of NCA-C_{18}-lys molecules, is assigned by the three Bragg peaks, $\{0,1\}_M$, $\{1,0\}_M$, and $\{1,-1\}_M$ that satisfy the requirement[29] in terms of the q_z maximum position of their corresponding Bragg rods (Figure 6a). The remaining Bragg peak, labeled HM, is attributed to a minor crystalline phase formed by the zwitterionic α-amino acid C_{18}-lys, (Scheme 1), generated via partial hydrolysis of the NCA-C_{18}-lys in contact with water.[30]

The derived unit cell of the major phase, of dimensions a = 4.9 Å, b = 5.6 Å, γ = 104°, area = 26.6 Å^2, contains one molecule with its hydrocarbon chain tilted by 44° from the normal to the surface, making an azimuth angle of 5° with the b^* reciprocal lattice vector (Scheme 3a). Thus the molecules in the 2-D crystal are related by translation symmetry. The

Scheme 3

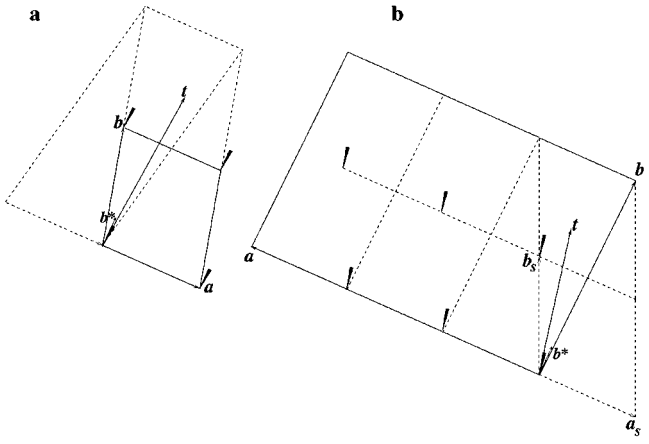

proposed molecular model was refined to give a reasonable fit between the observed and calculated Bragg rod intensity profiles (Figure 7a). The derived molecular packing arrangement, shown in Figure 7b−d, contains molecules linked by C═O···H−N hydrogen bonds along two different directions. One set, between the amide groups located within the hydrocarbon chains, runs along the a = 4.9 Å axis, whereas those between the anhydride five-membered rings lie along the unit cell diagonal $\boldsymbol{a}+\boldsymbol{b}$ (6.5 Å).[31] This network of hydrogen bonds can be considered as a

(29) Note that the three Bragg peaks belong to a single phase since the difference of the q_z positions of the intensity maxima of the $\{1,0\}_M$ and $\{0,1\}_M$ Bragg rods is equal to the q_z position of the intensity maximum of the $\{1,-1\}_M$ Bragg rod. This condition is required for long-chain amphiphiles.

(30) The HM Bragg peak matches the strongest reflection[13] measured from monolayers of C18-lys, and this α-amino acid was detected by MALDI-TOF MS analysis of samples taken from the water surface.

(31) Note that in the 3-D crystal structures of L-leucine-N^{α}-carboxyanhydride the N−H···O═C hydrogen bonds between the five-membered rings are formed along a 6.5 Å axis (see Kanazawa, H.; Kawai, T.; Ohashi, Y.; Sasada, Y. *Bull. Chem. Soc. Jpn.* **1978**, *51*, 2205).

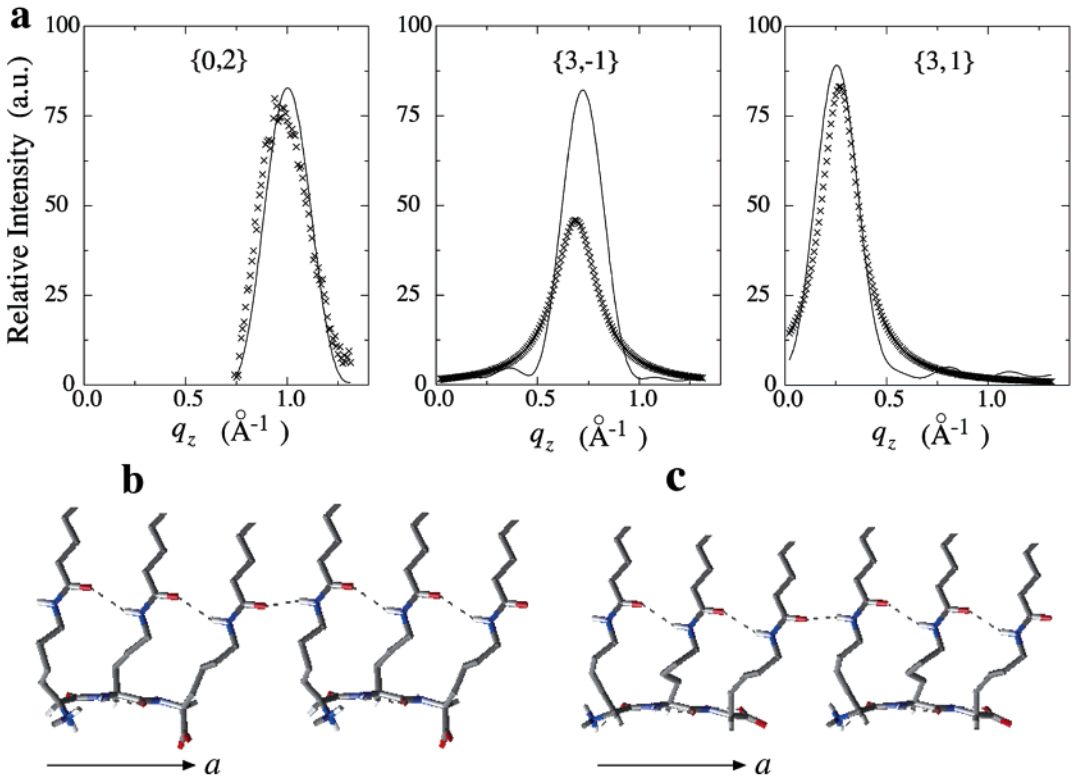

Figure 8. Structure determination of the product crystalline phase assuming a tripeptide molecule: (a) Measured (×) and calculated (—) Bragg rod intensity profiles, $I(q_z)$, of the {0,2}, {3,1}, and {3,−1} reflections corresponding to the pseudo-rectangular representation of the unit cell containing two tripeptide molecules, (b) proposed 2-D packing arrangement of tri-*SSS*-peptide molecules in the product mixture obtained from the polymerization of either enantiomeric or racemic NCA-C_{18}-lys viewed parallel to the water surface, and (c) tri-*RSR*-peptide molecule that would be accommodated in the same unit cell, respectively. For clarity only part of the hydrocarbon chains is shown.

driving force toward separation of (*R*,*S*)-NCA-C_{18}-lys molecules into enantiomorphous 2-D crystallites.

Monitoring the Polymerization in 2-D Crystallites of (*R*)- or (*S*)-NCA-C_{18}-lys by GIXD. Enantiomerically pure (*R*)- or (*S*)-NCA-C_{18}-lys spread on a nickel acetate aqueous solution at 4 °C (or 20 °C) for a nominal area of 35 Å^2 undergoes polymerization, as proven by kinetic GIXD measurements (see below) and the results of the MALDI-TOF MS analysis yielding oligopeptides containing up to 13 units. Thus the GIXD patterns (Figure 6b) measured from such monolayers show the self-assembled 2-D crystallites of the oligopeptide products. From the measured Bragg peaks, we derived an oblique "unit subcell" of dimension $a_s = 4.9$ Å, $b_s = 5.5$ Å, $\gamma_s = 114.6°$, area = 24.5 Å^2, containing one oligopeptide unit. Note that this subcell can be transformed into a centered pseudo-rectangular cell, $a = 4.9$ Å, $b = 9.9$ Å, $\gamma = 92.5°$ (Scheme 3b), containing two oligopeptide units. The hydrocarbon chains of the peptide units are tilted by 38° from the perpendicular to the surface, with an azimuth angle of 12° from the b^* reciprocal lattice vector (Scheme 3b), as derived from the measured Bragg rods. The length of the *a* axis is very similar to that of the (*R*)- or (*S*)-NCA-C_{18}-lys monomer phase. We propose that the polymerization reaction is constrained within the lattice imposed by the hydrogen-bonded hydrocarbon chains and proceeds across the *a* axis. The resulting oligopeptide molecules within the product lattice are constrained to have their intramolecular hydrocarbon chains parallel and separated by the hydrogen-bonding distance of 4.9 Å.

To provide evidence on the above process, we monitored the reaction by GIXD directly at the air−liquid interface. The effect of temperature was examined by spreading the (*R*)- or (*S*)-NCA-C_{18}-lys on a water subphase at room temperature. The GIXD pattern (Figure 6d) measured after cooling to 4 °C shows, in addition to the Bragg peaks of the starting monomer, weak Bragg peaks $\{0,1\}_P$, $\{1,0\}_P$, and $\{1,-1\}_P$ arising from the crystalline phase belonging to the oligopeptide product (Figure 6b). On the same sample preparation we next studied the effect of catalyst addition into the subphase. When a first portion of nickel acetate catalyst was injected into the subphase, a distinct increase in the intensity of the Bragg peaks of the oligopeptide crystalline phase $\{h,k\}_P$ and a concomitant decrease of those of the monomer phase $\{h,k\}_M$ were observed (Figure 6e). After injection of a second portion of catalyst, there was a complete disappearance of the starting monomer crystalline phase $\{h,k\}_M$ and an even larger increase in the intensity of the oligopeptide product phase $\{h,k\}_P$ (Figure 6f). The pattern of the product phase is very similar to that measured from the *(R)*- or (*S*)-NCA-C_{18}-lys monomer spread directly on the catalyst solution (Figure 6b). The gradual disappearance of the HM Bragg peak (Figure 6a,d,e), attributed to a hydrolyzed monomer phase, can be explained in terms of a solid−solution mixed phase formed between the oligopeptide products and the zwitterionic C_{18}-lys, all having free NH_3^+ and COO^- end groups.

We conclude from the above results that the (*R*)- or (*S*)-NCA-C_{18}-lys monomer molecules first self-assemble on the liquid surface and then undergo a catalyzed polymerization reaction. The oligopeptide product self-assembles into crystalline domains in which the molecular chains are related by translation. The crystalline solid-solution of oligopeptides, whose observed centered cell contains two repeat units, should be able to

accommodate a mixture composed of hydrolyzed monomer, di- and tripeptide molecules, in view of the MALDI-TOF-MS results (vide infra). This model was substantiated by X-ray structure-factor computations. Assuming a tripeptide product, we constructed a molecular model[32] containing three repeat units with parallel long hydrocarbon chains linked by intramolecular hydrogen bonds along the *a* axis. This model was refined in a unit cell of dimension $a_P = 3a$, $b_P = b$, $\gamma_P = \gamma$, to yield a reasonable fit between the observed and calculated Bragg rod intensity profiles (Figure 8a). The resulting packing arrangement (Figure 8b) contains the long hydrocarbon chains linked by intra- and intermolecular hydrogen-bonded ribbons along the a_P axis. Such a ribbon can be composed of a mixture of oligopeptides of different length with adjacent ribbons being randomly offset with respect to one another.

GIXD of (*R*,*S*)-NCA-C_{18}-lys. GIXD patterns measured from racemic (*R*,*S*)-NCA-C_{18}-lys amphiphiles, spread on either water or nickel acetate aqueous solutions at 4 °C and at 20 °C, show a single crystalline phase (Figure 6c), very similar to that of the oligopeptide product obtained from (*R*)- or (*S*)-NCA-C_{18}-lys when deposited on the aqueous solution of the catalyst. In view of the apparent high reactivity of the racemate, the GIXD measurements were additionally performed as quickly as possible, that is, within about 45 min after spreading the (*R*,*S*)-NCA-C_{18}-lys on water at 4 °C. Under these conditions, the GIXD pattern (Figure 9) displayed, in addition to the crystalline phase of the oligopeptide product (P), very weak Bragg peaks corresponding to small amount of the (*R*)- or (*S*)-NCA-C_{18}-lys monomer phase (M). When the sample was scanned after one more hour, the latter peaks were absent. A comparison between the diffraction patterns measured from various monolayers, before and after the injection of the catalyst, helps us to unequivocally assign the Bragg peaks belonging to either monomer or product crystalline phases (Figure 9). These results show that, according to GIXD, enantiomorphous crystalline domains were formed prior to the polymerization of (*R*,*S*)-NCA-C_{18}-lys monomer.

Composition of the Oligopeptide Products. According to the MALDI-TOF MS analysis on enantioselectively labeled samples prepared by polymerization of (*R*,*S*)-NCA-C_{18}-lys, a mixture of oligopeptide products containing up to six units and some hydrolyzed monomer is formed. The total amount of the oligopeptide products, deduced from the corresponding ion peak intensity, for each length in the range of $n = 2-6$ obtained under various conditions and normalized to the amount of dipeptides ($n = 2$) decreases exponentially as shown in Figure 10a.

For this system we assessed the extent of homochiral polymerization in a relative way by comparison with a reference state, to account for the presence of enantiomeric disorder and of amorphous material. As reference state, we use the decrease in crystalline order of the monolayer that occurs with increase in temperature. Thus, we compare the results of the MALDI-TOF MS analysis of the products obtained from the monolayer polymerization of (*R*,*S*)-NCA-C_{18}-lys at 4 °C (or 0 °C) with those obtained at 20 °C. The distribution of oligopeptides was determined from MALDI-TOF MS spectra measured using two different instruments in Rehovot and in Paris.

(32) The tri-*SSS*-peptide molecule, was constructed on the basis of the 3-D crystal structure of gly-gly-gly, see Srikrishnan, T.; Winiewicz, N.; Parthasarathy, R. *Int. J. Pept. Protein Res.* **1982**, *19*, 103.

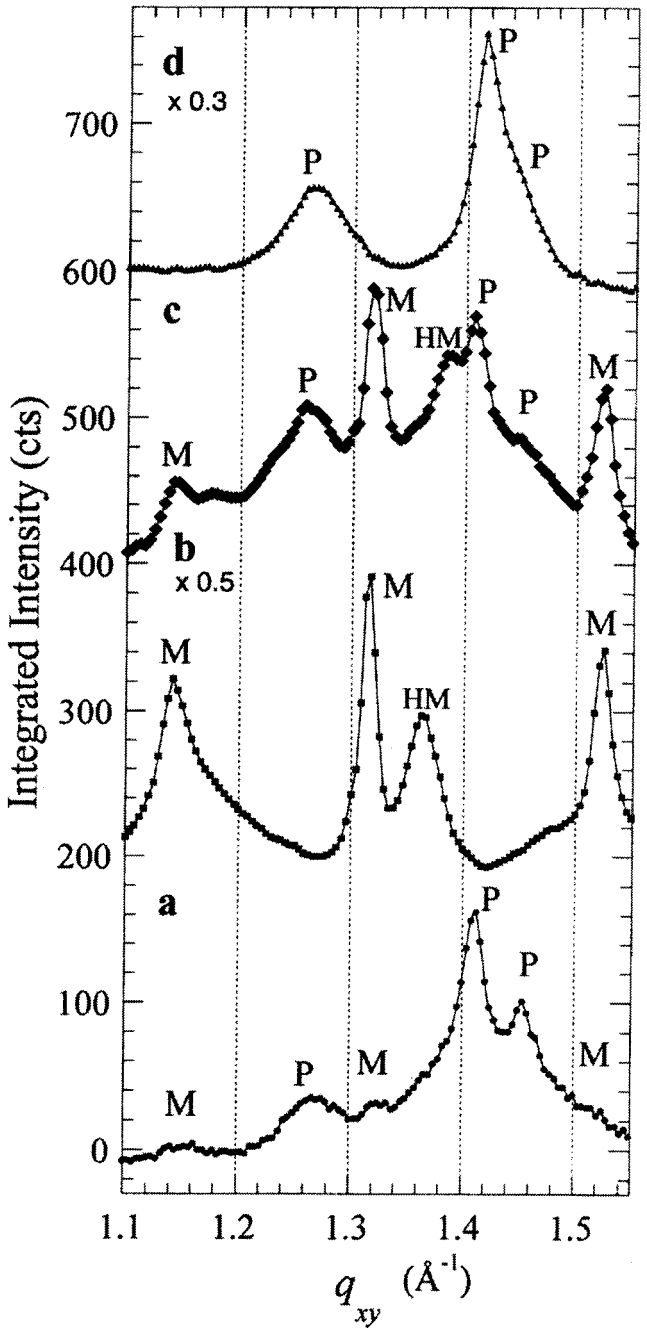

Figure 9. GIXD Bragg peaks, $I(q_{xy})$, measured from various monolayers: (a) (*R*,*S*)-NCA-C_{18}-lys, scanned in the shortest time possible, i.e., ~45 min after spreading the amphiphile solution on water at 4 °C, (b) (*R*)- or (*S*)-NCA-C_{18}-lys spread on water at 4 °C, (c) (*R*)- or (*S*)-NCA-C_{18}-lys spread on water at RT and cooled after 1 h to 4 °C (d) (*R*,*S*)-NCA-C_{18}-lys spread on water (as in (a) but later scans) or on catalyst aqueous solution at 4 °C, or as in (c) after injection of the catalyst into the water beneath the film.

The relative abundance of various oligopeptides with homochiral and heterochiral sequence up to hexapeptides obtained at 20 °C and 4 °C is presented in Figure 10b, and the excess calculated for the molecules with homochiral sequence [(*h*,0) + (0,*d*)] is shown in Figure 10d. The excess obtained from the polymerization reaction at 20 °C oscillates around unity, the value corresponding to a random process, in keeping with a fast polymerization reaction and low degree of order at this temperature. On the other hand, the results obtained at 4 °C and 0 °C indicate that whereas the excess of di- and tripeptides

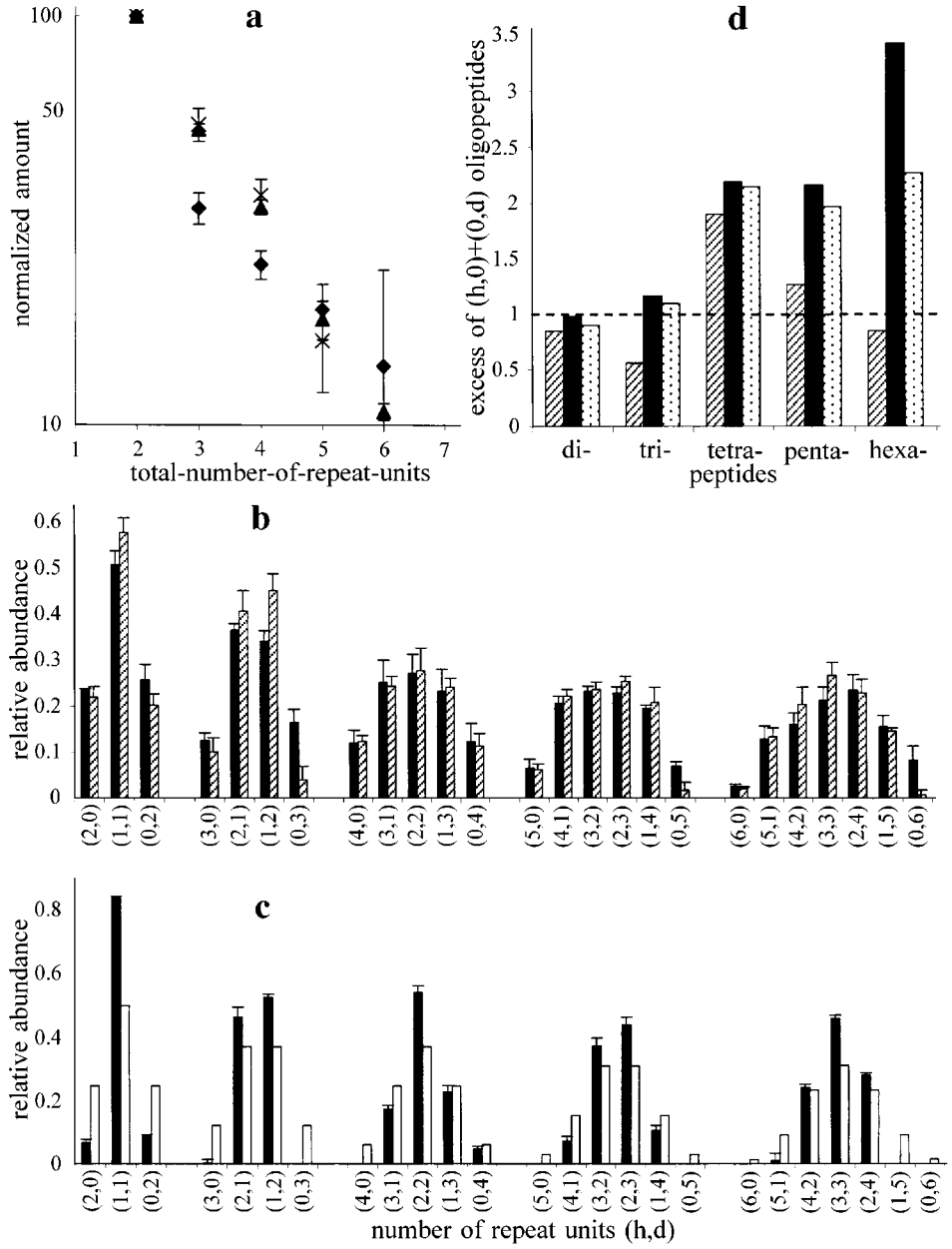

Figure 10. MALDI-TOF MS results: (a) Relative yield of the oligopeptides of various lengths, shown normalized to the dipeptide amount, as deduced from the corresponding ion intensity from various samples prepared from (*R*,*S*)-NCA-C_{18}-lys monomer at 20 °C on water (◆), at 4 °C on catalyst (▲), and at 4 °C with catalyst injection (×). Relative abundance of the oligopeptides obtained by polymerization at the air−aqueous solution interface of: (b) racemic (*R*,*S*)-NCA-C_{18}-lys and (c) racemic (*R*,*S*)-NCA-C_{18}-glu. The histogram in (b) shows the experimental results obtained at 4 °C (filled) and at 20 °C (lined). The histogram in (c) shows the experimental results obtained at 4 °C (filled) together with the theoretical values for a random process (unfilled); (d) The excess of oligopeptides with homochiral sequence [(*h*,0) + (0,*d*] is shown for the di- to hexapeptides obtained from the polymerization reactions of (*R*,*S*)-NCA-C_{18}-lys at 20 °C (lined), 4 °C (filled), and 0 °C (dotted). The horizontal dashed line represents an excess equal to unity.

with homochiral sequence is close to the value of one, the corresponding longer tetra-, penta-, and hexapeptides show an excess by a factor of 2 to 3.5. These results show indeed the tendency for the polymerization of (*R*,*S*)-NCA-C_{18}-lys to occur within the self-assembled enantiomorphous 2-D crystallites of the monomer. By contrast, a dramatic difference in the lattice-controlled polymerization is evident from the results obtained from a related monomer,[17] (*R*,*S*)-N^{α}-carboxyanhydride of γ-stearyl-glutamic acid, NCA-C_{18}-glu (Scheme 1) that self-assembles into a racemic 2-D crystal with the reaction occurring mainly between molecules of opposite handedness (Figure 10c). Thus, the distribution of the oligopeptides is center- rather than wing-weighted, namely heterochiral molecules were obtained with much higher relative abundance than the theoretical values.

The relative abundance of the oligopeptides with homochiral sequence obtained from the (*R*,*S*)-NCA-C_{18}-lys system is not as high as may be expected from a racemate self-assembling into enantiomorphous 2-D crystalline domains. Such behavior may be rationalized in terms of polymerization also occurring in the noncrystalline regions, at the periphery of the crystallites and at the line boundaries[33] between domains of opposite handedness. According to the width of the Bragg peaks of the

(33) Eckhardt, C. J.; Peachey, N. M.; Swanson, D. R.; Takacs, J. M.; Khan, M. A.; Gong, X.; Kim, J.-H.; Wang, J.; Uphaus, R. A. *Nature* **1993**, *362*, 614.

GIXD patterns, the enantiomorphous 2-D crystallites of the racemate have a smaller average size (~15−20 nm) than those formed from the enantiomerically pure amphiphiles (~30−50 nm). This difference in size implies that the ratio between the number of molecules at the periphery of the crystallites and the 2-D "bulk" is very different for the enantiomerically pure and racemic amphiphiles. According to the MALDI-TOF MS results, the oligopeptides obtained from enantiomerically pure amphiphiles are longer, containing up to 13 units. The formation of up to both homo- and heterochiral hexapeptides from the enantiomorphous domains of the racemate is consistent with their smaller average size and the presence of line boundaries. This result is not surprising since, from an energetic point of view, the initiation of the polymerization should be favored at the periphery of the domains. In addition, the crystallites are not isolated but rather form a continuous "membrane", as imaged by TEM on vitreous ice on related systems.[34] Therefore, we may envisage that the film is composed of alternating domains of opposite handedness related by pseudo-mirror symmetry. At these line boundaries, the reaction is faster, resulting in heterochiral di- and tripeptides. Note that heterochiral di- or tripeptide can be easily accommodated within the 2-D lattice of the product phase[35] (Figure 8c). Nevertheless, the excess of tetra- to hexapeptides with homochiral sequence (Figure 10d) can be rationalized as being due to a lattice-control polymerization within the "bulk" of the enantiomorphous domains.

Conclusions

The central message of the present study bears on the interplay between the molecular two-dimensional arrangement of racemic monomer amphiphiles that separate into enantiomorphous domains comprising molecules of single handedness, at the air−water interface and the stereochemistry of the oligopeptide products obtained by lattice-controlled reaction. It proved possible to obtain oligopeptides with homochiral sequences in a higher relative abundance than that obtained at increased temperature or from a theoretical random process. By contrast, closely related molecules that self-assemble into a racemic type of 2-D crystallites yielded primarily heterochiral oligopeptides due to reaction occurring between molecules related by glide symmetry.

Structured clusters of water-soluble, hydrophobic, natural α-amino acids can be formed at the air−solution interface[36,37] or even within the bulk of aqueous solutions. Thus, the higher relative abundance of homochiral oligopeptides obtained in aqueous solutions from racemic NCA-derivatives of tryptophan, leucine, and isoleucine reported by Hitz et al.[38] might have arise from polymerization occurring within structured clusters.

The present approach is being extended for the generation of homochiral oligopeptides of single handedness starting from chiral nonracemic mixtures of monomers.

The role played by stereospecific interactions between amphiphilic molecules in the formation of 2-D crystallites on liquid or solid surfaces might provide rational routes in transforming racemic monomers into homochiral biopolymers at prebiotic times

Experimental Section

Materials. (*R*)-, (*S*)-, and (*R,S*)-N^{α}-carboxyanhydride of N^{ϵ}-stearoyl-thio-lysine (NCA-C_{18}-lys) were synthesized from the corresponding long-chain amino acid N^{ϵ}-stearoyl lysine (C_{18}-lys), according to a reported procedure.[39] (*R*)-, or (*S*)-, and (*R,S*)-N^{ϵ}-stearoyl-thio-lysine (C_{18}-thio-lys) were obtained from the corresponding NCA-C_{18}-lys with H_2S in the presence of 2,6-lutidine at −10 °C.[40] C_{18}-lys, was synthesized by the reaction between with *N*-hydroxysuccinimide of stearic acid and (*R*)-, (*S*)-, and (*R,S*)-lysine, according to standard procedures. For the normal series of compounds, we used stearic acid (purchased from Aldrich) and for deuterated compounds we used perdeuterated stearic acid (D35 98% purchased from Cambridge Isotope Laboratories).

Characterization of compounds: (*R*)-, (*S*)-, (*R,S*)-NCA-C18-lys ($C_{17}H_{35}$-chain): ^{1}H NMR (400 MHz) δ 0.94 (t, 3H), 1.2−1.5 (br m 28H), 1.6−1.9 (br m 6H), 2.2−2.4 (br m 2H), 2.26 (t 2H), 3.2−3.4 (m 2H), 4.36 (t 1H) 5.72 (s 1H); FTIR (KBr pellet) 3328, 2919, 2851, 1864, 1821, 1762, 1642, 1532, 1472, 1089, 945 cm-1; ESMS m/z = 437.2 $[M - H]^-$.

(*R*)-, (*S*)-, (*R,S*)-NCA-C_{18}-lys ($C_{17}D_{35}$-chain): ^{1}H NMR (400 MHz) δ 1.6 (m 4H), 2.2 (br m 2H), 3.2−3.4 (t 2H), 4.35 (t 1H) 5.6 (s 1H); FTIR (KBr pellet) 3328, 2944w, 2859w, 2196, 2085, 1864s, 1830vs, 1770s, 1642, 1523, 1089, 1328, 1089, 945 cm^{-1}; ESMS m/z = 472.7 $[M - H]^-$.

C_{18}-thio-lys ($C_{17}H_{35}$-chain): ^{1}H NMR (400 MHz) δ 0.9 (t, 3H), 1.2−1.5 (br m 28H), 1.6−1.9 (br m 6H), 2.2−2.4 (br m 2H), 2.75 (t 2H), 3.64 (t 2H), 4.62 (t 1H, characteristic for the H linked to the asymmetric C atom of an amino thio acid); FTIR (KBr pellet) 3319, 2919, 2851, 1642, 1591, 1532, 1472 cm^{-1}; ESMS m/z = 429.2 $[M + H]^+$, 451.2 $[M + Na]^+$.

C_{18}-thio-lys ($C_{17}D_{35}$-chain): ^{1}H NMR (400 MHz) δ 1.6−1.9 (br m 4H), 2.2−2.4 (br m 2H), 3.7 (t 2H), 4.67 (t 1H); FTIR (KBr pellet) 3328, 2920w, 2859w, 2196, 2085 1642, 1591, 1523, 1413, 1327, 1089 cm^{-1}; ESMS m/z = 464.7 $[M + H]^+$, 486.6 $[M + Na]^+$. As catalysts, we used nickel acetate·$4H_2O$ (purchased from Aldrich), I_2/KI prepared by dissolution of 1.9 g (7.5 mmol) crystalline I_2 (purchased from Merck) into an aqueous solution of KI (4 g = 24 mmol in 60 mL of H_2O) and $AgNO_3$ (purchased from Aldrich).

Sample Preparation. The solutions (0.5 mM) of the amphiphile monomers were prepared in chloroform, neat for NCA-C_{18}-lys or containing 1% TFA for C_{18}-thio-lys. These solutions were spread on the surface of pure water or other aqueous subphases, at 4 °C, for a nominal molecular area (area of the trough divided by the total number of molecules contained in the spreading solution) of 35 $Å^2$, corresponding to ~75% monolayer coverage. Under these conditions, the surface pressure did not increase above 1 mN/m. GIXD measurements were performed on such samples after purging with cold helium. The polymerization reactions were performed on samples prepared on pure water surface followed by addition of the appropriate catalyst. The polymerization of NCA-C_{18}-lys was initiated by injecting the catalyst (50 mL of concentrated aqueous solution of nickel acetate, reaching a final concentration of 5 mM) beneath the 2-D crystallites self-assembled on pure water at 0, 4, and 20 °C. The reaction time was 2 h. The polymerization of C_{18}-thio-lys was induced by injection of 15 mL of I_2/KI aqueous solution to reach a final concentration of 1 mM, and the reaction time was 2−4 h.

(34) Popovitz-Biro, R.; Majewski, J.; Margulis, L.; Cohen, S.; Leiserowitz, L.; Lahav, M. *Adv. Mater*. **1994**, *98*, 956.
(35) There are small differences in the dimensions of the unit cell (a = 4.9 Å b = 9.9−10.0 Å, γ = 90.5−92.5°) derived from the GIXD patterns of product phase obtained from enantiomerically pure monomers and from racemic mixtures of monomers, spread on water and then catalyst addition or on catalyst containing subphase.
(36) Weissbuch, I.; Addadi, L.; Berkovitch-Yellin, Z.; Gati, E.; Lahav, M.; Leiserowitz, L. *Nature* **1984**, *310*, 161.
(37) Weissbuch, I.; Leiserowitz, L.; Lahav, M. *J. Am. Chem. Soc*. **1991**, *113*, 8941.
(38) Hitz, T.; Blocher, M.; Walde, P.; Luisi, P. L. *Macromolecules* **202**, *34*, 2443.
(39) Daly, W. H.; Poché, D. *Tetrahedron Lett.* **1988**, *29*, 5859.
(40) Cricchio, R.; Berti, M.; Cietto, G.; DePaoli, A. *Eur. J. Med. Chem.* **1981**, *16*, 301.

MALDI-TOF MS. After the reaction, the monolayer films were compressed with the barrier, and the material, observed by visual inspection, was collected from the liquid surface, transferred to a glass vial, and dried under vacuum. Samples for the MALDI-TOF MS analysis were then prepared by dissolving the dry material in chloroform containing 1% trifluoroacetic acid. One microliter of this solution was deposited on top of a matrix deposit (dithranol containing NaI) on the instrument holder. The MALDI-TOF positive ion mass spectra were obtained in reflector mode from two different instruments at the Weizmann Institute (Bruker Biflex 3) and at the University of Paris VI (Perseptive Biosystems, Voyager Elite), both equipped with a N_2 laser. External calibration of the mass spectra was achieved using calibrating peptide (substance P, ACTH 8-39) in the studied mass range. Only singly charged ions, $(M + H)^+$, $(M + Na)^+$, and $(M + 2Na - H)^+$ with the expected isotopic pattern, were observed. Other ions with the same isotopic pattern were often observed and shifted by $\Delta m/z$ of 4 units and 6 units with respect to $(M + Na)^+$ and $(M + 2Na - H)^+$, presumably resulting from gas phase reaction of these species. The nature of these ions is currently under investigation. In these experiments, the isotopic pattern for a given oligomeric species containing protonated and deuterated units and the mass precision (better than 0.1 unit) are sufficiently well defined to correctly assign the monomer composition of the various observed ions. Mass spectra resulted from an signal average of at least a few hundred laser shots in different spots of the target to get a reliable statistic about the ion peak. The good statistic is obtained when the isotopic distribution of an ion species corresponds to that expected. Mass assignments were made using both *m*/*z* measurement and isotopic distribution (different from protonated and deuterated monomers). A good agreement was found on both instruments for the observed ions and their relative abundance.

We use the following notation code of the oligopeptide molecules: (*h*,*d*) designates a molecule comprising *h S*(protonated) repeat units and *d R*(deuterated) repeat units, with $n = h + d$, being the total number of repeat units.

The relative abundance (r.a.) of each type of oligopeptide (*h*,*d*) is obtained by dividing the intensity of all the ions from a particular molecule to the total intensity of the ions from all the molecules of the same length, *n*. For example, the relative abundance of the tetrapeptide (4,0) composed of four *S*(protonated) chains, is calculated with the following equation:

$$\text{r.a.}(4,0) = \text{intensity}(4,0)/\text{intensity}\{(4,0) + (3,1) + (2,2) + (1,3) + (0,4)\}$$

In addition, we calculate the excess of oligopeptides with homochiral sequence by normalizing the experimental relative abundance of these oligopeptides $[(h,0) + (0,d)]$ to the corresponding value calculated assuming a binomial distribution of *R* and *S* repeat units.

$$\text{excess}[(h,0) + (0,d)] = [\text{r.a.}(h,0) + \text{r.a.}(0,d)]_{\text{exp}}/[\text{r.a.}(h,0) + \text{r.a.}(0,d)]_{\text{theoretical}}$$

The theoretical values of the relative abundance (r.a.) calculated for a binomial distribution of the *R* and *S* repeat units in an oligopeptide (*h*,*d*) is given below in the table:

(*h*,*d*)	r.a.	(*h*,*d*)	r.a.
(2,0)	0.25	(5,0)	0.03125
(1,1)	0.50	(4,1)	0.15625
(0,2)	0.25	(3,2)	0.3125
(3,0)	0.125	(2,3)	0.3125
(2,1)	0.375	(1,4)	0.15624
(1,2)	0.375	(0,5)	0.03125
(0,3)	0.125	(6,0)	0.01562
(4,0)	0.0625	(5,1)	0.09375
(3,1)	0.25	(4,2)	0.23438
(2,2)	0.375	(3,3)	0.3125
(1,3)	0.25	(2,4)	0.23438
(0,4)	0.0625	(1,5)	0.09375
		(0,6)	0.01562

GIXD measurements were performed using the liquid-surface diffractometer mounted at the BW1 synchrotron beamline at Hasylab, DESY, Hamburg. Details about the experimental technique and the instrument were reported elsewhere.[6] The measured GIXD patterns are represented as two-dimensional contour maps of the scattered intensity, $I(q_{xy}, q_z)$, as a function of the horizontal q_{xy} and vertical q_z components of the scattering vector. The unit cell dimensions of the 2-D lattice are derived from the q_{xy} positions of the Bragg peaks. The full width at half-maximum of the Bragg peaks (corrected for instrument resolution), fwhm (q_{xy}), gives an estimate of the crystalline coherence lengths $L_{hk} \approx 0.9(2\pi/\text{fwhm}(q_{xy}))$ associated with each *h*,*k* reflection. Bragg rod intensity profiles represent the intensity distribution along q_z, $I(q_z)$, derived by integrating across the q_{xy} range for each of the Bragg peaks. The full width at half-maximum of the Bragg rod intensity profiles, fwhm (q_z), gives an estimate of the thickness $d \approx 0.9(2\pi/\text{fwhm}(q_z))$ of the 2-D crystallites The intensity at a particular value of q_z in a Bragg rod is determined by the square of the molecular structure factor $|F_{h,k}(q_z)|^2$. The 2-D packing arrangement is determined by performing X-ray structure factor calculations, using atomic coordinate molecular models constructed using the CERIUS[2] molecular package, and rigid-body structure refinement, using the SHELX-97 program adapted for 2-D structures.

Acknowledgment. We thank the Israel-Science Foundation, the Petroleum Research Fund of the American Chemical Society, and the Danish Foundation for Natural Sciences for financial support. H.Z. thanks the Swiss Foundation, the G. M. J. Schmidt Minerva Center for Supramolecular Architectures, and the Crown Genome Centre for a postdoctoral fellowship. This work was supported by the IHP-Contract HPRI-CT-1999-00040 of the European Community. We are grateful to HASYLAB at DESY, Hamburg, for beam time at the BW1 beamline.

JA0259943